Indian Journal of Chemistry
Vol. 64, April 2025, pp. 361-372
DOI: 10.56042/ijc.v64i4.14872

A new approach for the synthesis of strobilurin fungicide analogues: Synthesis, characterization, antifungal study and molecular docking investigation

Nagashree U Hebbar[a], Arpita A Shanbhag[a], Lokesh A Shastri[a]*, Smita Shinde[b], Umashri Jambale[c], Shivasharana C T[c], Sudhesh L Shastri[d] & Vijaykumar K N[e]

[a] Department of Chemistry, Karnatak University, Dharwad 580 003, Karnataka, India

[b] Department of Botany, Karnatak University, Dharwad 580 003, Karnataka, India

[c] Department of Biotechnology and Microbiology, Karnatak University, Dharwad 580 003, Karnataka, India

[d] Department of Biotechnology Kuvempu University, Shivamogga 577 451 Karnataka, India

[e] Department of Plant Pathology, UAS, Dharwad 580 005, Karnataka, India

E-mail: drlashastri@kud.ac.in

Received 6 November 2024; accepted (revised) 26 March 2025

In an effort to protect plants from fungal diseases and to enhance the stability of the strobilurin fungicides, we report herein, an efficient and simple approach for the synthesis of strobilurin fungicide analogues. The synthesised compounds were characterised by IR, NMR and LC-MS spectroscopic techniques. The antifungal efficacies of the synthesised compounds were tested against plant pathogens namely *Curvularialunata*, *Rhizoctonia solani* and *Sclerotium rolfsii* by using poison food/pour plate and spore germination methods. *Azoxystrobin* and *Tebuconazole* are used as standards in the analysis. Further, the synthesized compounds were subjected to *in silico* studies to know the bonding interactions with bovine cytochrome Bc1 and CYP51 protein of cytochrome 450.

Keywords: Strobilurin fungicide, Plant pathogens, Poison food plate, Spore germination, Molecular docking

Plant pathogenic fungi are one of the leading causes of crop loss. A precise pest control strategy is needed in order to minimize environmental risks along with enhancing agricultural production in order to meet the demands of a continually expanding population[1]. One of the most significant families of contemporary pesticides for crops is the strobilurin fungicides[2]. Strobilurins are naturally occurring compounds derived primarily from mushrooms (*basidiomycetes*). Their name comes from the fungus genus *Strobilurus*. The methyl (E)-3-methoxy-2-(5-phenylpenta-2,4-dienyl) acrylate moiety was present in all naturally occurring strobilurins[3]. The field usage of the natural strobilurins is not feasible due to challenges in their large-scale manufacturing, relative volatility, and photochemical instability. The developments of synthetic strobilurins were made possible by separate research attempts carried out by Syngenta and BASF. Azoxystrobin and kresoxim-methyl (Fig. 1) were the earliest strobilurins to enter the market in 1996 (Ref. 4,5). The primary characteristic of strobilurin fungicides in terms of structure is the presence of a toxiphoric (*E*)-methoxyacrylate group. Yet, this group was substituted with QSAR-equivalent units in several synthetic strobilurin fungicides[6]. Most of the natural as well as the synthetic strobilurins that are registered so far share an aromatic bridge that gives the molecule photochemical stability with a unique bulky substituent in the *ortho* position along with toxophoric group[7]. Some of the marketed strobilurins are listed in Fig. 1. Coumarin is extensively found in natural products, pharmaceuticals, and agrochemicals as the structural core. Osthol, a naturally occurring O-methylated coumarin discovered in *Cnidium Monnieri*, which exhibited wide range of distinct pathogenic fungi, particularly against *Rhizoctonia solani*. Interestingly, coumoxystrobin and coumethoxystrobin (Fig. 1), are newly created fungicide with broad-spectrum fungicidal activity against numerous plant diseases, by combining two bioactive components of coumarin and methoxy acrylate into a single molecule[8-10].

Considering the resistance of fungal strains to the existing fungicides and the instability of strobilurin fungicides towards light and heat, we designed and synthesised our target molecule having similar

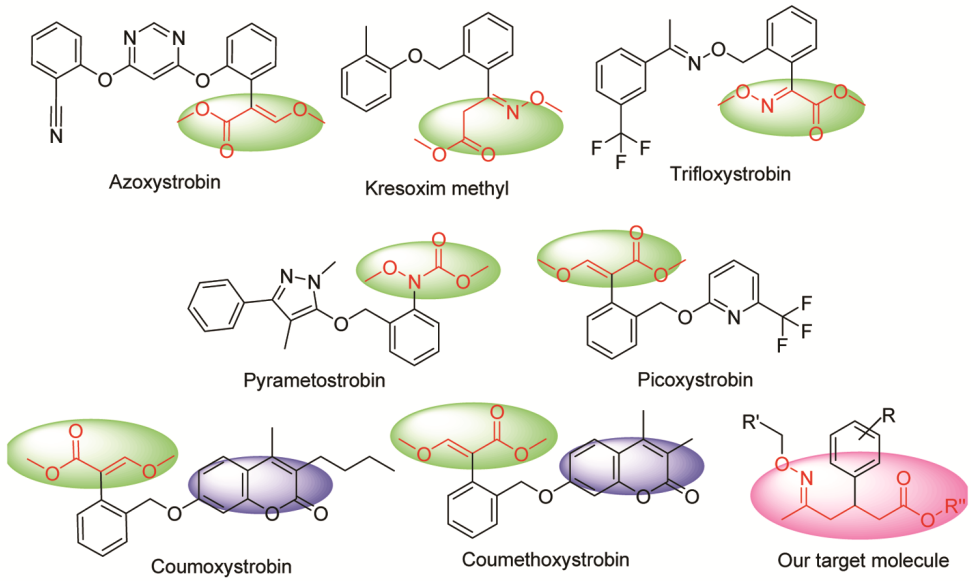

Fig. 1 — Some of the market-based strobilurin fungicides and our target molecule

pharmacophore unit as that of strobilurins containing oxyimino hexanoic and hexanoate derivatives with benzyl or methyl coumarin substitution at oxygen of oxyimino group and tested them for their antifungal efficacy against plant pathogens namely *Sclerotium rolfsii*, *Rhizoctonia solani* and *Curvularia lunata* by poison food/ pour plate and spore germination methods. Then subjected to *in silico* molecular docking studies to know the bonding interactions with cytochrome bc1 and CYP51 of cytochrome P450 enzyme.

Experimental Section

The melting points were determined using open capillary method and are uncorrected. On a Nicolet IN-10 FTIR spectrophotometer, IR spectra (KBr disc) were recorded. The ^{1}H and ^{13}C NMR spectra were recorded using a Jeol 400 and 100 MHz spectrometer with $CDCl_3$ as the solvent. LC-MS/ESI-MS-Waters ACQUITY TQD was used to collect mass spectra. All the reagents were of analytical grade and used as received.

General procedure for synthesis of 5-((substituted oxyimino)-3-(4-substituted aryl)hexanoic acid, 7a-f

The synthesized beta aryl oxo hexanoic acid derivative **5a-c** (1mmol) and the methyl oxy amine compounds **6a-b** (1.2 mmol) were dissolved in methanol (5 mL) catalytic amount of TEA is added and kept for stirring at RT until the reaction is complete as determined by TLC (ethyl acetate: hexane: 2:8). Then the reaction mixture was poured into ice-cold water and the separated solid was filtered, washed with water and recrystallized from methanol to yield substituted methyl oxy imino hexanoic acid derivatives **7a-f.**

5-((Benzyloxy)imino)-3-(4-nitrophenyl)hexanoic acid, 7a: White solid. Yield 88%. m.p.90-92°C. FT-IR (KBr): 1721 cm^{-1} (C=O); ^{1}H NMR (400 MHz, $CDCl_3$): δ 1.79 (s, 3H, CH_3), 2.44-2.75 (m, 4H, CH_2), 3.55 (m, 1H, CH), 4.98 (s, 2H, OCH_2), 7.18-7.20 (m, 2H, Ar-H), 7.25-7.32 (m, 5H, Ar-H), 8.03-8.07 (m, 2H, Ar-H); ^{13}C NMR (101 MHz, $CDCl_3$): δ 14.9, 38.5, 40.0, 41.8, 75.4, 123.8, 127.7, 128.4, 146.9, 150.4, 154.9, 177.2; EI-MS: *m/z* Calcd for $C_{19}H_{20}N_2O_5$: 356.38. Found: 357.2 [M+1].

5-((Benzyloxy)imino)-3-(4-fluorophenyl)hexanoic acid, 7b: White solid. Yield 87%. m.p.86-88°C. FT-IR (KBr): 1719 cm^{-1} (C=O); ^{1}H NMR (400 MHz, $CDCl_3$): δ 1.72 (s, 2H, CH_3), 2.40-2.65 (m, 4H, CH_2), 3.45 (m, 1H, CH), 4.92 (s, 2H, OCH_2), 7.12 (d, J = 8.2 Hz, 2H, Ar-H), 7.21-2.29 (m, 7H, Ar-H); ^{13}C NMR (101 MHz, $CDCl_3$): δ 15.0, 38.6, 40.2, 42.0, 74.9, 115.3, 127.8, 128.6, 129.9, 139.0, 139.7, 156.1, 178.3; EI-MS: *m/z* Calcd for $C_{19}H_{20}FNO_3$: 329.37. Found: 330.3 [M+1].

5-((Benzyloxy)imino)-3-(4-chlorophenyl)hexanoic acid, 7c: White solid. Yield 88%. m.p.88-90°C. FT-IR (KBr): 1718 cm^{-1} (C=O); ^{1}H NMR (400 MHz, $CDCl_3$): δ 1.81 (s, 3H, CH_3), 2.41-2.69 (m, 4H, CH_2), 3.42 (m, 1H, CH), 5.18 (s, 2H, OCH_2), 7.08 (d, J = 8.2 Hz, 3H, Ar-H), 7.20-7.25 (m, 4H, Ar-H), 7.29-

7.34 (m, 2H, Ar-H); ^{13}C NMR (101 MHz, $CDCl_3$): δ 14.9, 38.5, 40.8, 42.4, 76.0, 128.0, 128.6, 130.0, 132.6, 141.7, 156.1, 179.7; EI-MS: *m/z* Calcd for $C_{19}H_{20}ClNO_3$: 345.82. Found: 346.1 [M+1].

3-(4-Nitrophenyl)-5-(((6-methyl-2-oxo-2*H*-chromen-4-yl)methoxy)imino)hexanoic acid, 7d: White solid. Yield 94%. m.p.182-184°C. FT-IR (KBr): 1726 (C=O),1703 cm^{-1} (C=O); ^{1}H NMR (400 MHz, $CDCl_3$): δ 1.82 (s, 3H, CH_3), 2.41 (s, 3H, Coum-CH_3), 2.44-2.72 (m, 4H, CH_2), 3.60 (m, 1H, CH), 5.12 (s, 2H, OCH_2), 6.18 (s, 1H, CH), 7.21-7.25 (m, 2H, Ar-H), 7.35 (d, J = 9.2 Hz, 3H, Ar-H), 8.11 (d, J = 9.2 Hz, 2H, Ar-H); ^{13}C NMR (101 MHz, $CDCl_3$): δ 14.7, 21.3, 39.1, 40.8, 42.2, 71.0, 117.0, 118.1, 120.6, 129.3, 132.1, 134.0, 141.4, 151.2, 157.5, 160.8, 178.7; EI-MS: *m/z* Calcd for $C_{23}H_{22}N_2O_7$: 438.44. Found: 439.1 [M+1].

3-(4-Fluorophenyl)-5-(((6-methyl-2-oxo-2*H*-chromen-4-yl)methoxy)imino)hexanoic acid, 7e: Light yellow solid. Yield 92%. m.p.140-142°C. FT-IR (KBr): 1723 (C=O), 1701 cm^{-1} (C=O); ^{1}H NMR (400 MHz, $CDCl_3$): δ 1.86 (s, 3H, CH_3), 2.38 (s, 3H, Coum-CH_3), 2.50-2.68 (m, 4H, CH_2), 3.43 (q, J = 7.1 Hz, 1H, CH), 5.15 (s, 2H, OCH_2), 6.30 (s, 1H, CH), 6.92 (t, J = 8.6 Hz, 2H, Ar-H), 7.08-7.12 (m, 2H, Ar-H), 7.21-7.33 (m, 3H, Ar-H); ^{13}C NMR (101 MHz, $CDCl_3$): δ 14.9, 21.1, 38.0, 40.6, 42.4, 70.7, 112.9, 115.4, 115.7, 117.1, 117.3, 123.5, 128.8, 128.8, 132.9, 134.2, 151.7, 152.0, 157.7, 161.6, 176.3; EI-MS: *m/z* Calcd for $C_{23}H_{22}FNO_5$: 411.43. Found: 412.1 [M+1].

3-(4-Chlorophenyl)-5-(((6-methyl-2-oxo-2*H*-chromen-4-yl)methoxy)imino)hexanoic acid, 7f: Grey solid. Yield 94%. m.p.122-124°C. FT-IR (KBr): 1717 (C=O), 1687 cm^{-1} (C=O); ^{1}H NMR (400 MHz, $CDCl_3$): δ 1.81 (s, 3H, CH_3), 2.39 (s, 3H, Coum-CH_3), 2.44-2.68 (m, 4H, CH_2), 3.44 (m, 1H, CH), 5.18 (s, 2H, OCH_2), 6.18 (s, 1H, CH), 6.71-6.96 (m, 3H, Ar-H), 7.10-7.21 (m, 4H, Ar-H); ^{13}C NMR (101 MHz, $CDCl_3$): δ 14.6, 21.5, 38.6, 40.6, 42.0, 70.8, 113.1, 115.4, 115.7, 117.0, 123.5, 128.7, 132.8, 134.1, 138.7, 150.4, 151.5, 157.6, 160.7, 161.2, 179.3; EI-MS: *m/z* Calcd for $C_{23}H_{22}ClNO_5$: 427.88. Found: 428.6 [M+1].

General procedure for synthesis of 5-((6-methylcoumarin 4-methoxyimino)-3-(4-substituted aryl)hexanoate, 8d-f

The hexanoic acid derivatives **7** obtained was dissolved in methanol and stirred at RT in the presence of 1 drop of sulphuric acid catalyst until the completion of reaction according to TLC (ethyl acetate: hexane: 2:8). Then the reaction mixture is poured into ice-cold water, formed precipitate was filtered and recrystallised from methanol to obtain hexanoate derivatives **8a-f**.

Methyl-5-((benzyloxy)imino)-3-(4-nitropheny) hexanoate, 8a: White solid. Yield 92%. m.p.62-64°C. FT-IR (KBr): 1730 cm^{-1} (C=O); ^{1}H NMR (400 MHz, $CDCl_3$): δ 1.80 (s, 3H, CH_3), 2.44-2.71 (m, 4H, CH_2), 3.56 (s, 4H, CH, CH_3), 4.98 (s, 2H, OCH_2), 7.19-7.29 (m, 7H, Ar-H), 8.05 (d, J = 7.6 Hz, 2H, Ar-H); ^{13}C NMR (101 MHz, $CDCl_3$): δ 14.8, 38.8, 40.2, 41.8, 51.8, 75.4, 123.8, 127.7, 127.8, 128.3, 128.4, 138.3, 146.8, 150.7, 154.8, 171.9; EI-MS: *m/z* Calcd for $C_{20}H_{22}N_2O_5$: 370.41. Found: 371.1 [M+1].

Methyl-5-((benzyloxy)imino)-3-(4-fluorophenyl) hexanoate, 8b: White solid. Yield 90%. m.p.56-58°C FT-IR (KBr): 1730 cm^{-1} (C=O); ^{1}H NMR (400 MHz, DMSO-d_6): δ 1.69 (s, 3H, CH_3), 2.38-2.62 (m, 2H, CH_2), 3.37 (d, J = 46.5 Hz, 5H, CH_2, CH_3), 4.90 (s, 2H, OCH_2), 7.12 (m, 9H, Ar-H); ^{13}C NMR (101 MHz, DMSO-d_6): δ 14.9, 38.5, 42.0, 51.7, 74.9, 115.3, 127.8, 128.6, 129.9, 139.0, 139.7, 156.1, 172.3; EI-MS: *m/z* Calcd for $C_{20}H_{22}FNO_3$: 343.40. Found: 344.3 [M+1].

Methyl-5-((benzyloxy)imino)-3-(4-chlorophenyl) hexanoate, 8c: Light brown solid. Yield 90%. m.p.60-62°C. FT-IR (KBr): 1733 cm^{-1} (C=O); ^{1}H NMR (400 MHz, $CDCl_3$): δ 1.79 (s, 3H, CH_3), 2.39-2.66 (m, 4H, CH_2), 3.42 (m, 1H, CH), 3.56 (s, 3H, CH_3), 5.01 (s, 2H, OCH_2), 7.08 (d, J = 8.2 Hz, 3H, Ar-H), 7.20-7.25 (m, 4H, Ar-H), 7.29-7.34 (m, 2H, Ar-H); ^{13}C NMR (101 MHz, $CDCl_3$): δ 14.7, 38.6, 40.5, 42.2, 51.7, 75.4, 127.6, 128.4, 128.8, 132.5, 141.2, 155.7, 172.4; EI-MS: *m/z* Calcd for $C_{20}H_{22}ClNO_3$: 359.85. Found: 360.1 [M+1].

Methyl-5-(((6-methyl-2-oxo-2*H*-chromen-4-yl) methoxy)imino)-3-(4-nitrophenyl) hexanoate, 8d: Grey solid. Yield 90%. m.p.110-112°C. FT-IR (KBr): 1733 (C=O), 1710 cm^{-1} (C=O); ^{1}H NMR (400 MHz, $CDCl_3$): δ 1.88 (s, 3H, CH_3), 2.39 (s, 3H, Coum-CH_3), 2.48-2.62 (m, 2H, CH_2), 2.68-2.74 (m, 2H, CH_2), 3.57-3.62 (m, 4H, CH, OCH_3), 5.14 (s, 2H, OCH_2), 6.20 (s, 1H, CH), 7.21-7.25 (m, 1H, Ar-H), 7.32 (d, J = 8.2 Hz, 4H, Ar-H), 8.09 (d, J = 8.2 Hz, 2H, Ar-H); ^{13}C NMR (101 MHz, $CDCl_3$): δ 14.9, 21.1, 38.4, 40.9, 41.9, 51.9, 70.8, 113.0, 117.1, 120.8, 129.1, 131.8, 134.0, 141.7, 151.6, 157.3, 161.1, 172.2; EI-MS: *m/z* Calcd for $C_{24}H_{24}N_2O_7$: 452.46. Found: 453.3 [M+1].

Methyl-3-(4-fluorophenyl)-5-(((6-methyl-2-oxo-2*H*-chromen-4-yl)methoxy)imino) hexanoate, 8e: White solid. Yield 89%. m.p.108-110°C. FT-IR (KBr): 1730 (C=O), 1709 cm^{-1} (C=O); ^{1}H NMR (400 MHz, $CDCl_3$): δ 1.84 (s, 3H, CH_3), 2.40 (s, 3H, Coum-CH_3), 2.46-2.64 (m, 4H, CH_2), 3.39, (q, J = 7.1 Hz, 1H, CH), 3.58 (s, 3H, OCH_3), 5.21 (s, 2H, OCH_2), 6.29 (s, 1H, CH), 7.05-7.17 (m, 4H, Ar-H), 7.22-7.35 (m, 3H, Ar-H); ^{13}C NMR (101 MHz, $CDCl_3$): δ 14.8, 21.4, 38.5, 40.8, 42.0, 52.1, 70.9, 113.3, 114.4, 114.9, 116.7, 117.3, 124.5, 128.2, 130.2, 133.5, 134.7, 152.7, 153.6, 157.7, 161.0, 171.9; EI-MS: *m/z* Calcd for $C_{24}H_{24}FNO_5$: 425.46. Found: 426.3 [M+1].

Methyl-3-(4-chlorophenyl)-5-(((6-methyl-2-oxo-2*H*-chromen-4-yl)methoxy)imino) hexanoate, 8f: White solid. Yield 88%. m.p.116-118°C. FT-IR (KBr): 1735 (C=O), 1714 cm^{-1} (C=O); ^{1}H NMR (400 MHz, $CDCl_3$): δ 1.84 (s, 3H, CH_3), 2.37 (s, 3H, Coum-CH_3), 2.41-2.55 (m, 2H, CH_2), 2.60-2.66 (m, 2H, CH_2), 3.42 (m, 1H, CH), 3.55 (s, 3H, OCH_3), 5.14 (s, 2H, OCH_2), 6.26 (s, 1H, CH), 6.89-6.96 (m, 2H, Ar-H), 7.08-7.15 (m, 2H, Ar-H), 7.23 (m, 2H, Ar-H), 7.31 (d, J = 7.8 Hz, 1H, Ar-H); ^{13}C NMR (101 MHz, $CDCl_3$): δ 14.8, 21.1, 38.4, 40.8, 42.1, 51.8, 70.8, 113.1, 115.4, 115.7, 117.0, 123.5, 128.7, 132.8, 133.9, 138.3, 151.4, 151.8, 157.5, 160.5, 161.1, 172.3; EI-MS: *m/z* Calcd for $C_{24}H_{24}ClNO_5$: 441.91. Found: 442.8 [M+1].

Antifungal assay

Poisoned food technique

The antifungal activity of synthesized compounds was tested on plant fungal pathogens namely *Sclerotium rolfsii*, *Curvularialunata* and *Rhizoctonia solani* using poisoned food technique[11] by analyzing the mycelial growth inhibition efficiency of the test samples. In 100 mL autoclaved media, 25 mg of samples dissolved in 250µL Acetone was added and immediately transferred to petri plates and kept to solidify. Azoxystrobin and Tebuconazole were exploited as reference drugs. The cultured test fungi's 6 mm diameter mycelia mass was placed in the exact centre of each plate independently to inoculate the test fungal species. The petri plates were kept at RT for 7 to 10 days, or until the control petri plates' mycelial mass had almost completely filled the plate. Averaging the radical growth of the mycelia mass in orthogonal directions yielded the diameter of the growth mass, and the percentage of inhibition was estimated using the formula[12].

Percentage of inhibition

$$I = \frac{C - T}{C} \times 100$$

Where C denotes the average diameter of mycelial growth in the control sample and T denotes the average diameter of mycelial growth in the test sample.

Spore germination technique

To examine the *in vitro* spore germination in *Sclerotium rolfsii* indigenous technology knowledge (ITK) was used[13,14] at a concentration of 100 mg L^{-1} of test samples in acetone and distilled water. The suspension of Matured sclerotial bodies along with suspension of test samples were placed on top of cavity slides kept in a petri dish lined with moistened blotter paper using distilled water and incubated at 28°C. Three replications were made in each treatment. The spore germination was evaluated under microscope after 48 h of incubation. The formula provided by Vincent[12] was used to compute sclerotial germination as well as the percent suppression of sclerotial germination.

$$I = \frac{C - T}{C} \times 100$$

Where C is no of seeds germinated in control and T is no of seeds germinated in test sample.

Molecular Docking

The crystal structure of the target bovine B cytochrome-1 (Bovine Bc1) and CYP51 protein were extracted from Protein Data Bank (PDB ID; 1SQB). Using Chem Draw Ultra 12.0, the structures of synthesised compounds **7a-f**, **8a-f**. Azoxystrobin and clotrimazole were drawn. PRODRG online platform[15] was used to retrieve 3D coordinates. The CASTp webserver was used to identify active pockets for proteins[16]. Energy minimization, protein and ligand preparation, and grid box generation were all performed using the graphical user interface programme Auto Dock Tools (ADT). The prepared file was saved in PDBQT format by Auto Dock. Leveraging protein and ligand information as well as grid box attributes from the configuration file, Auto Dock/Vina was applied for docking, which use iterated local search global optimizer[17,18]. Both the protein and the ligands are regarded to be rigid during the process of docking. Positional root-mean-square deviation (RMSD) less than 1.0 was placed together and corresponding to the result with the lowest free energy of binding. For further investigation, the orientation

with the lowest binding energy or affinity was extracted and aligned with the receptor structure[19,20].

Results and Discussion

Chemistry

The title strobilurin analogue targets **7a-f** and **8a-f** have been synthesized by the reaction of beta aryl oxohexanoic acid **5a-c**[21]. The methyloxy amine derivatives **6** were reacted with oxohexanoic acid derivatives **5a-c** at RT in methanol leading to the formation of Schiff's bases of hexanoic acids **7a-f**, the reaction rate can be enhanced with the presence of one drop of triethyl amine (TEA). Further, the methyl hexanoate derivatives **8a-f** were achieved by the esterification reaction of compounds **7a-f** in methanol (Scheme 1). The structures of all the synthesized compounds are depicted in Fig. 2 and all the molecules were subjected to spectral analysis to validate the formation of the proposed structures.

The obtained spectral data of the compounds were in good agreement with the anticipated structures. In IR spectrum of compound **7a**, the carbonyl stretching frequency is observed at 1721 cm^{-1}. In ^1H NMR spectrum, the methyl protons attached to carbon adjacent to imine carbon resonated as singlet at δ 1.79 ppm and the four methylene protons resonated as multiplet from δ 2.44 to 2.75 ppm. The quintet

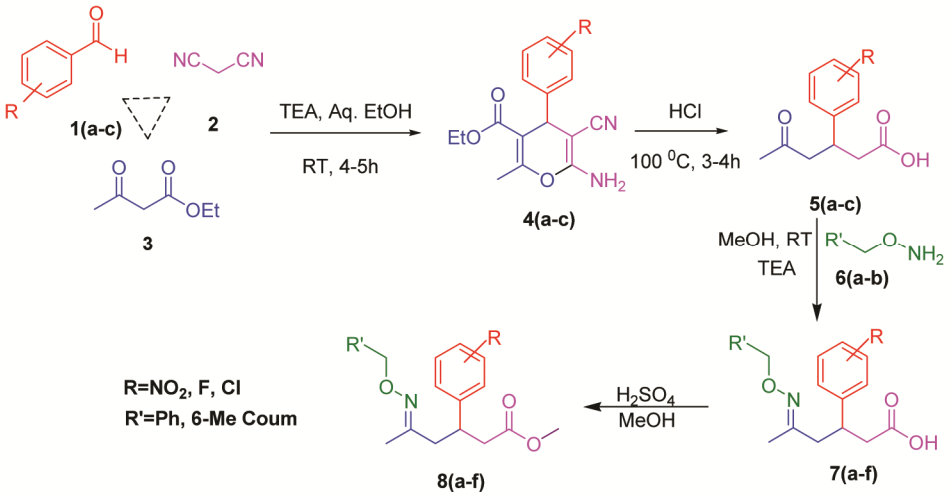

Scheme 1 — Synthesis of strobilurin analogues **7a-f** and **8a-f**

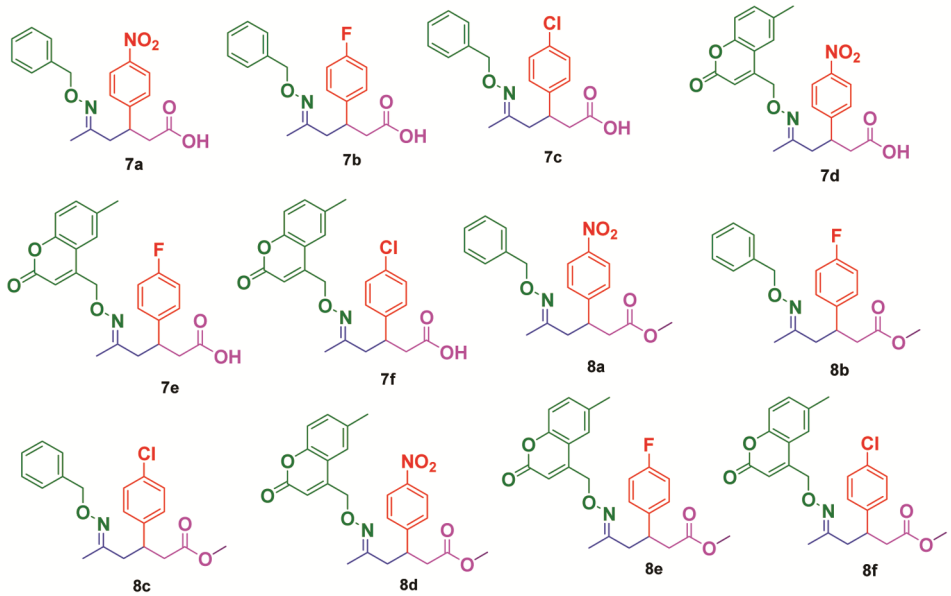

Fig. 2 — Structures of all the synthesized compounds **7a-f** and **8a-f**

corresponding to one proton at δ 3.55 ppm represented methine proton. Whereas, the singlet at δ 4.98 ppm represented methylene protons adjacent to oxygen. The remaining peaks from δ 7.18 to 8.07 ppm represented aromatic protons and the ^{13}C NMR peaks are well in agreement with the predicted structure of **7a**. Further, the structure of **7a** was confirmed by mass analysis which showed the (M+1) *m/z* peak at 357.

Similarly, compound **8f** was confirmed by spectral analysis, IR stretching band of ester carbonyl observed at 1735 cm^{-1}. In ^{1}H NMR spectrum of compound **8f**, the singlet at δ 1.84 ppm denotes methyl protons of carbon adjacent to imine carbon and the singlet at δ 2.37 ppm signifies methyl protons of coumarin ring. The methylene protons adjacent to carbonyl and imine carbons resonated as multiplet at δ 2.41-2.66 ppm. While the methylene protons adjacent to oxygen resonated as singlet at δ 5.14 ppm. The quintet at δ 3.42 ppm corresponded to methine proton and the singlet at δ 3.55 ppm corresponding to three protons denotes ester methyl group. The C_3-H proton of coumarin ring resonated as singlet at δ 6.26 ppm. The remaining peaks from δ 6.89 to 7.31 ppm are due to seven aromatic protons. Wherein, all the carbons resonated in ^{13}C NMR spectrum is in the respective region. The *m/z* peak at 442.19 in LC-MS corresponded to the (M+1) of the compound **8f**.

Antifungal activity

Food poison technique

The antifungal activity of samples was tested on a plant pathogen namely *Curvularialunata* and *Rhizoctonia solani*. The analysis was carried out by poison food/ pour plate method[11] and the obtained results are displayed in Table 1 and the PDA plates indicating percentage inhibition is shown in Fig. 3. Azoxystrobin a strobilurin fungicide and

Table 1 — Antifungal activity results of compound **7a-f** and **8a-f**

Compd	*Curvularia lunata*		*Rhizoctonia solani*	
	ZOI (cm)	% of Inhibition	ZOI (cm)	% of Inhibition
7a	3.38	42.8	0.06	0.70
7b	3.83	48.5	0.12	1.55
7c	3.16	40.0	0.00	0.00
7d	0.87	11.1	0.00	0.00
7e	1.52	19.2	0.02	0.28
7f	2.88	36.4	0.09	1.13
8a	1.37	17.4	0.30	3.80
8b	1.97	25.0	0.12	1.55
8c	3.77	20.2	0.14	1.83
8d	2.83	47.8	0.04	0.56
8e	3.25	41.2	0.01	0.14
8f	2.97	37.6	0.36	4.50
Control	NA	NA	NA	NA
Acetone Control	NA	NA	NA	NA
Azoxystrobin	7.27	92.0	7.90	100.00
Tebuconazole	1.6	2.10	7.79	100.00

*Control- untreated PDA plates.
*Acetone control- PDA plates treated with acetone.

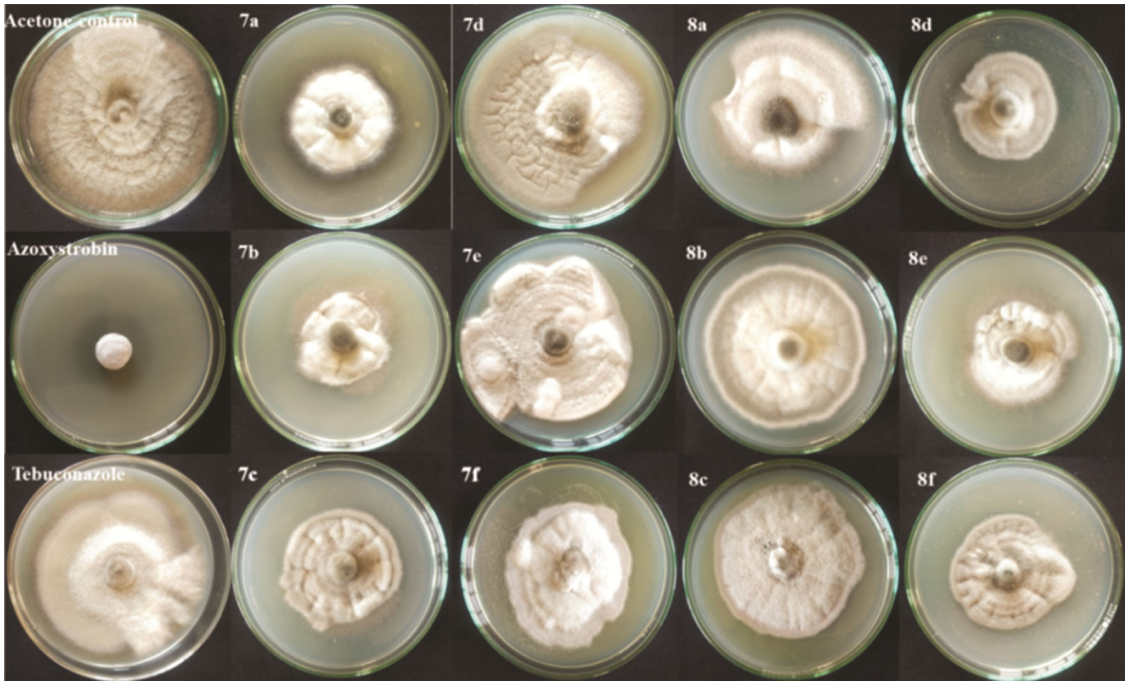

Fig. 3 — PDA plates indicating the degree of inhibition of *Curvularialunata* with tested samples **7a-f, 8a-f** and standards on 12th day of inoculation

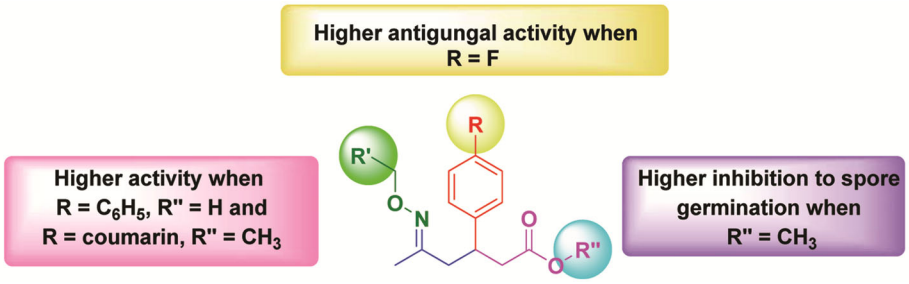

Fig. 4 — Brief structure activity relationship (SAR) of antifungal activity against *Curvularia lunata* and *scelotium rolfsi*

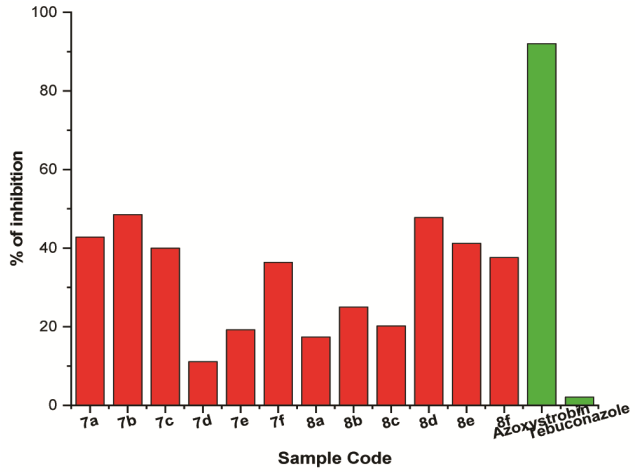

Fig. 5 — Graphical representation of antifungal activity against *Curvularialunata*

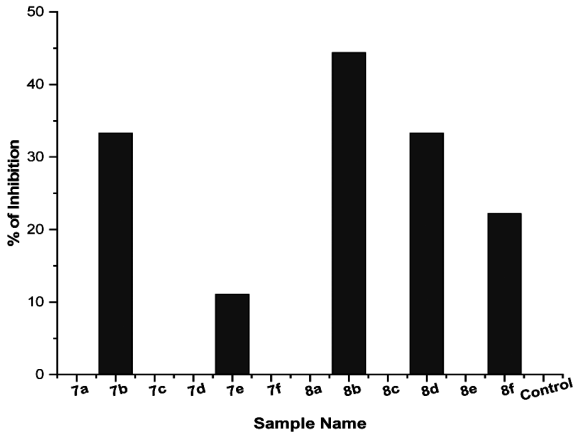

Fig. 6 — Graphical representation of spore germination efficiency against *scelotiumrolfsi*

Taboconazole a azole-based fungicide was used as standards. The analysis was carried out at the concentration of 250 mg $L^{-1}$and acetone was used as the solvent. The synthesised compounds have shown very good activity against *Curvularialunata*. Compound **7b** with flouro substitution on phenyl ring has shown good inhibition activity and the benzyl oxyimino substituted acidic compounds **7a-c** have shown higher activity compared to others. Among these, compound **8d** with nitro substitution on phenyl ring has shown highest activity. The coumarin substituted hexanoate derivatives **8d-f** have shown higher activity. A brief structure activity relationship is shown in Fig. 4. The standard tebuconazole didn't show inhibition of *Curvularialunata*. The activity results are represented graphically in Fig. 5. The compounds have shown very less or no activity against *Rhizoctonia solani.*

Spore germination technique

Strobilurin fungicides are said to be highly effective against spore germination rather than the fungal mycelium[22]. Hence, the inhibition of early-stage spore germination of *scelotiumrolfsi* was assessed for the synthesised compounds **7a-f** and **8a-f** at the concentration of 100 mg L^{-1}. The obtained results are summarised in Table 2 and presented graphically in Fig. 6. Compound hexanoate derivative **8b** with flouro substitution on phenyl ring has shown good inhibition effect compared to others. Compounds **7b** and **8d** also have shown good inhibition efficacy.

Table 2 — Results obtained from spore germination method against *Scelotium rolfsi*

Compd	No. of sclerotial bodies	No. of germinated sclerotial bodies	% of Inhibition
Control	9	9	0.0
Acetone Control	9	9	0.0
7a	9	9	0.0
7b	9	6	33.3
7c	9	9	0.0
7d	9	9	0.0
7e	9	8	11.1
7f	9	9	0.0
8a	9	9	0.0
8b	9	5	44.4
8c	9	9	0.0
8d	9	6	33.3
8e	9	9	0.0
8f	9	7	22.2

*Control- untreated spores.
*Acetone control- spores treated with acetone.

Molecular Docking

In fungi, the strobilurins operate by preventing mitochondrial respiration. They inhibit the transport of electrons from cytochrome b to cytochrome c1 by binding to the Q_o site on cytochrome b. This stops the generation of ATP, which cuts off the internal energy cycle in fungi because of this they are also known as the Q_oI fungicides[23]. Hence, the synthesized compounds were docked into the active site of bovine B cytochrome-1(Bovine Bc1)(PDB ID: 1SQB). The docking results are summarized in Table 3. The results reveal that the compounds have similar inhibition efficiency compared to the standard drug in relation to the target, Bovin Bc1 protein.

Fig. 7 shows the ligplot analysis and docking results of compound **7b** in the crystal structure of bovine Bc1. It is seen that the compound **7b** makes one hydrogen bonding interaction with the protein which is raised from the fluorine atom of **7b** with the hydrogen atom of Tyr273 (F---H-Tyr273, 2.92 Å). Here the amino

Table 3 — Molecular docking interactions of compounds **7a-f** and **8a-f** with bovine Bc1 protein (PDB ID: 1SQB)

Compd	Affinity (kcal/mol)	No. of H-bonds	H-bond length (Å)	H-bond with amino acids	Hydrophobic interactions with amino acids
Azoxystrobin	–10.8	1	3.12	Glu271	Phe128, Tyr273, Ala127, Val132, Ser139, Ala143, Tyr131, Pro270, Gly142, Lys269, Met138, Phe274, Ile146, Tyr278, Met124, Ala125
7a	–8.9	–	–	–	Leu294, Val291, Ala295, Ile146, Phe128, Glu271, Tyr131, Ala127, Phe274, Pro270, met124, Ala277
7b	–9.5	1	2.92	Tyr273	Ala127, Phe274, Ala125, Met124, Ile146, Pro270, tyr278, Gly142, Lys269, Met138, Phe128, Tyr131, Glu271
7c	–8.9	1	2.63	Thr336	Leu333, Ile92, Trp272, Met96, Tyr95, Phe276, Val98, Leu332, Val329
7d	–9.5	1	2.89	Thr336	Leu333, Trp272, Ile92, Met96, Val329, Tyr95, Leu301, Val98, Leu120, Phe276, Leu332
7e	–10.1	1	2.63	Thr336	Leu333, Ile92, Trp272, Met96, Tyr95, Val98, Phe276, Leu332, Val329
7f	–10.1	–	–	–	Ile298, Ala125, Phe128, Ile146, Ile268, Gly142, Pro270, Met138, Glu271, Tyr131, Tyr278, Tyr273, Lys269, Ala127, Phe276, Ala277, Met124, Phe274
8a	–9.1	–	–	–	Tyr273, Pro270, Glu271, Ile146, Phe128, Tur278, Ala277, Leu281, Phe128, Leu294, Ala125, Met124, Phe274, Ala127, Tyr131
8b	–9.2	–	–	–	Ala277, Leu294, Ile146, Pro270, Glu271, Tyr273, Tyr131, Phe128, Ala127, Met124, Phe274
8c	–9.1	–	–	–	Leu121, Leu294, Ile146, Phe274, Met124, Ala125
8d	–9.6	–	–	–	Leu301, Leu120, Tyr95, Leu332, Thr336, Trp272, Leu333, Ile92, Val329, Met96, Phe276, Val98
8e	–8.0	–	–	–	Ala295, Leu121, Val291, Ile146, Ala125, Leu294, Met124, Phe128, Phe274, Ala277
8f	–9.8	–	–	–	Ile298, Ile146, Ile268, Pro270, Tyr278, Gly142, Lys269, Phe128, Tyr131, Ala127, Glu271, Tyr273, Phe274, Met138, Ala277, Met124, Leu294

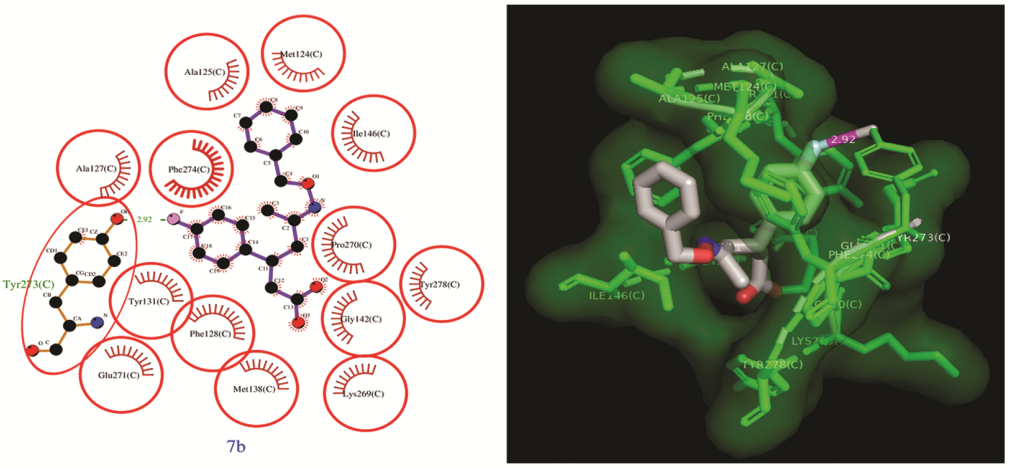

Fig. 7 — The crystal structure of bovine Bc1 protein (PDB ID: 1SQB) with the ligand **7b**

acids surrounding compound **7b** are same as the amino acids surrounding the standard azoxystrobin (similar amino acids are marked within red circle).

The ligplot analysis and docking results of compound **7e** with crystal structure of bovine Bc1 is depicted in Fig. 8 which shows one hydrogen bonding interaction from oxygen of oxyimino group of **7e** with Thr336 (O---H-Thr336, 2.63 Å). Here the amino acids surrounding the compound **7e** are different from the amino acids surrounding the reference azoxystrobin.

Fig. 9 indicates the ligplot analysis and docking outcomes of the reference drug azoxystrobin with the crystal structure of bovine Bc1, where one hydrogen bonding interaction is seen from carbonyl oxygen of azoxystrobin with the hydrogen of Glu271 (O---H-Glu271, 3.12 Å). The surrounding amino acids which are common in both azoxystrobin and compound **7b** are marked within red circle. In general, the synthesised compounds have very good interaction with the target protein and the site of interactionsare similar to that of the standard drug azoxystrobin.

Ergosterol is structurally distinct from the sterols found in animals and plants, and it plays a significant role in modulating the permeability and flexibility of fungal cell membranes. The cytochrome P450 enzyme lanosterol 14α-demethylase (CYP51) catalyses the formation of ergosterol, which preserves the firmness and viability of the membranes of fungi. As the ergosterol biosynthesis stops, the fungal cell membranes quickly degrade, which ultimately leads to death of fungi. Hence, the enzyme sterol 14α-demethylase (CYP51) is the target of antifungal drugs[24,25]. The synthesized compounds were docked into the active site of membrane protein CYP51 (PDB ID: 6UW2) and the

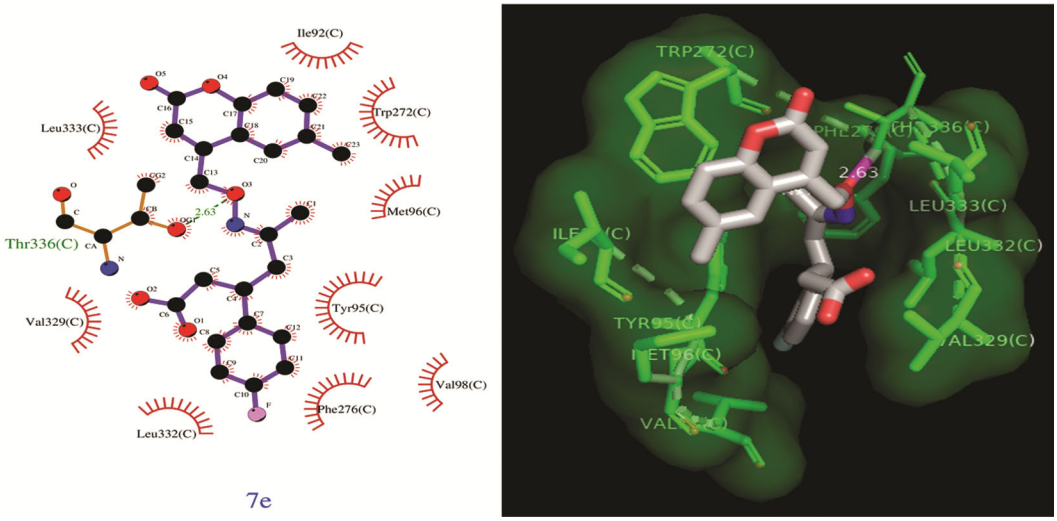

Fig. 8 — The crystal structure of bovine Bc1 protein (PDB ID: 1SQB) with the ligand **7e**

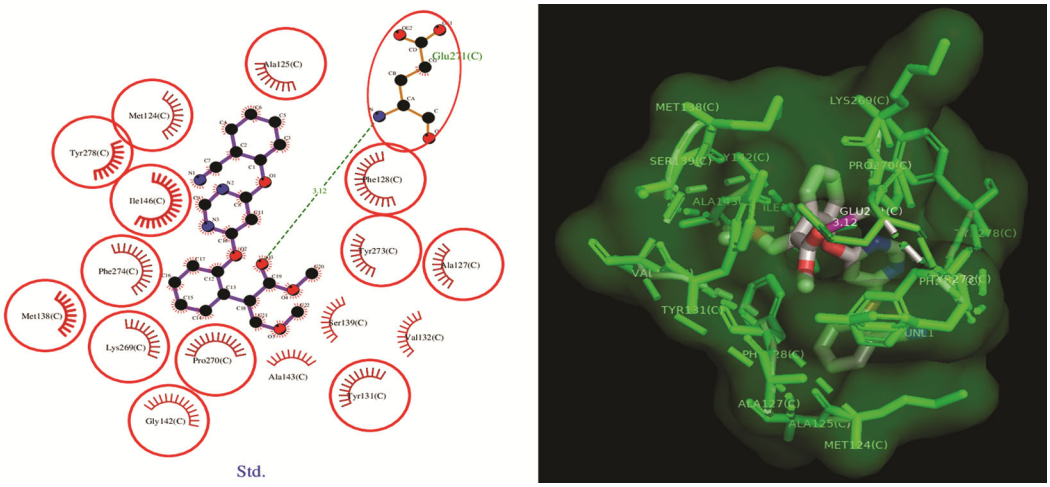

Fig. 9 — The crystal structure of bovine Bc1 protein (PDB ID: 1SQB) with the standard azoxystrobin

docking results are summarised in Table 4. The docking score reveals that the compounds have very good affinity with the target protein and some have shown better hydrogen bonding interactions.

The ligplot analysis and docking results of the compound **7d** are shown in Fig. 10. The compound makes seven hydrogen bonding interactions, among which four interactions are from carbonyl oxygen of compound **7d** with the amino acids Gln110, Arg368 and Tyr114 (O---H-Gln110, 3.22 Å, O---H-Arg368, 2.99 and 3.00 Å, O---H-Tyr114, 3.13 Å), two interactions were from oxygen of carboxylic acid group with Gln110 and Tyr127 (O---H-Gln110, 3.28 Å and O---H-Tyr127, 2.71 Å). The remaining one interaction is from nitrogen of imine group with Tyr127 (N---H-Tyr127, 3.04 Å). Fig. 11 depicts the docking analysis of compound **8d** where one hydrogen bonding interaction is observed. The interaction is from oxygen of nitro group with the Thr302 (O---H-Thr302, 2.97 Å).

The standard drug clotrimazole didn't show hydrogen bonding interaction but has good energy of affinity as shown in Fig. 12. The hydrophobic

Table 4 — Molecular docking interactions of compounds **7a-f** and **8a-f** with protein CYP51 (PDB ID: 6UW2)

Compd	Affinity (kcal/mol)	No. of H-bonds	H-bond length (Å)	H-bond with amino acids	Hydrophobic interactions with amino acids
Clotrimazole	–8.4	–	–	–	Ala290, Tyr127, Val126, Phe116, Tyr114, Phe121, Phe293, Ala294, Thr298
7a	–8.3	2	2.77 3.00	Gly426 Thr302	Ser299, Ala440, Cys434, Gly428, Leu363, Phe116, Tyr127, Tyr114, Val366, Phe427, Leu357
7b	–7.7	4	2.89 3.04 3.06 3.13	Tyr127 Arg368 Gln110	Tyr114, Phe365, Phe116, leu363, val126, Ile141, Leu291, Leu138, Val366
7c	–7.9	1	3.21	Thr302	Ala440, Phe427, Pro362, Ala290, Phe293, Ala294, Phe121, His297, Leu363, Gly426, Cys434, Thr298
7d	–8.9	7	3.04 2.71 3.28 3.22 3.00 2.99 3.13	Tyr127 Gln110 Arg368 Tyr114	Phe365, Ile141, Leu291, Val126, Ala290, Phe121, Met367, Phe116, Leu363, Val366
7e	–8.3	2	2.88 3.01	Ala470 Tyr468	Leu50, Pro64, Val473, Leu364, Phe365, Met471, Met367, Val221, Phe222, Phe60, Thr469
7f	–7.9	–	–	–	Leu50, Thr469, Ala470, Phe60, Pro64, Phe222, Pro218, Met471, Val221, Met367, Phe116, Phe365, Tyr468, Leu364
8a	–8.3	1	3.03	Thr302	Ala440, Ser299, Thr298, Cys434, Tyr114, Phe116, Tyr127, Pro391, Leu363, Gly428, Gly426, Leu357, Phe427, Pro362
8b	–7.4	–	–	–	Tyr127, Phe121, Leu363, Phe116, Ser117, Phe293, Ala294, Ala290, Thr298, Phe365, Leu216, Tyr114
8c	–9.8	–	–	–	Phe60, Phe222, Gln86, Leu88, Val83, Met367, Val221, Leu50, Phe365
8d	–9.5	1	2.97	Thr302	Ala440, Phe427, Cys434, Gly426, Gly428, Thr298, Val366, Pro362, Phe121, Tyr127, Phe116, Leu216, His297, Ala294, Leu363, Phe293, Ser299, Leu357
8e	–7.9	–	–	–	Leu50, Pro64, Val473, Ala470, Leu364, Val221, Met367, Phe222, Phe60, Met471, Phe365, Tyr468, Thr469
8f	–8.6	–	–	–	Val366, Tyr127, Phe116, Ser117, Phe293, Leu216, Ile120, His297, Leu363, Ala290, Phe121, Thr298, Ala294, Tyr114

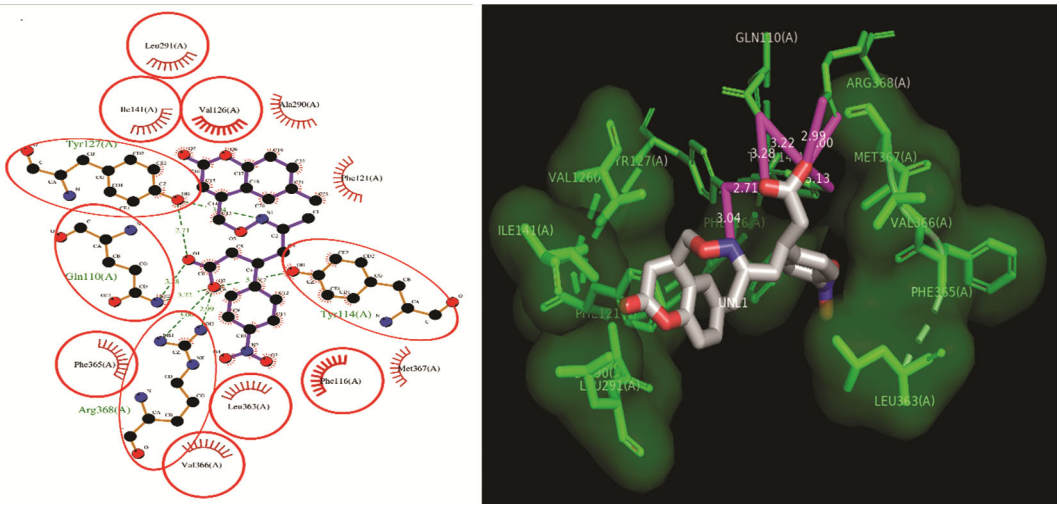

Fig. 10 — The crystal structure of protein CYP51 (PDB ID: 6UW2) with the ligand **7d**

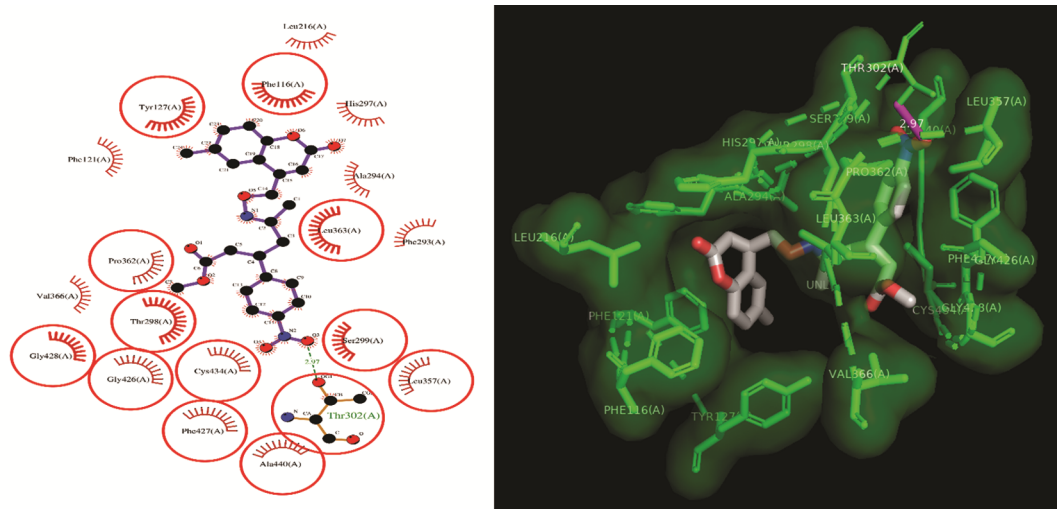

Fig. 11 — The crystal structure of protein CYP51 (PDB ID: 6UW2) with the ligand **8d**

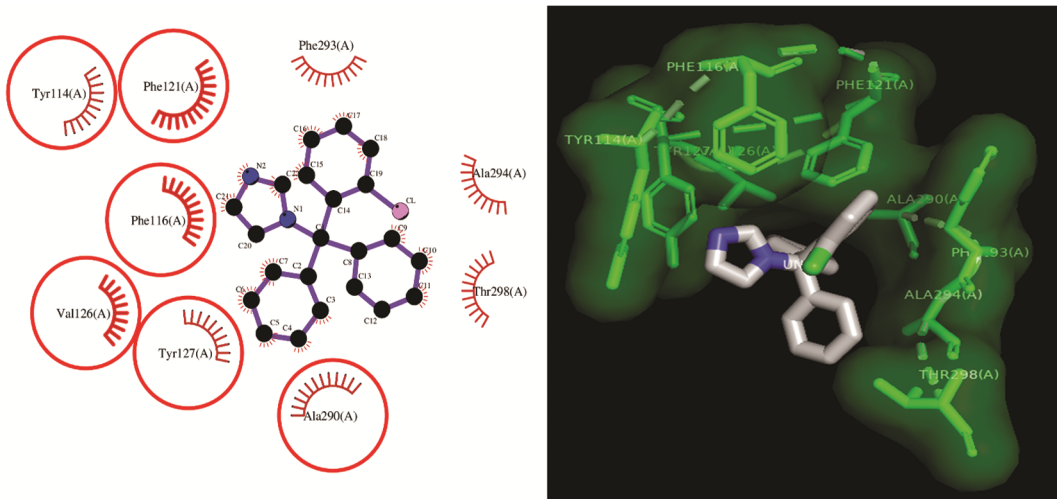

Fig. 12 — The crystal structure of protein CYP51 (PDB ID: 6UW2) with the standard drug clotrimazole

interactions are shown and the common amino acids surrounding the drug are shown within red circle.

Conclusions

A series of strobilurin analogues were synthesized using simple synthetic procedure and characterized by IR, NMR and mass spectroscopic techniques. Synthesized scaffolds were assayed for their antifungal activity against plant pathogens, and the inhibition activity results of the synthesised samples were higher against *Curvularialunata* and moderate against *Sclerotium rolfsii,* while lowest against *Rhizoctonia solani*. The *in silico* studies are revealed that the molecules have very good interaction with the bovine Bc1 protein (PDB ID; 1SQB) and CYP51 (PDB ID: 6UW2) protein with good affinity.

Conflict of interests

The authors declare that they have no conflict of interest.

Acknowledgements

One of the authors Nagashree U Hebbar, acknowledges University Grants Commission for providing CSIR-UGC fellowship (Ref. No. 191620123081, Roll. No. KK1016200804, Dated: 20/07/2020). Authors also thank the University Scientific Instrumentation center (USIC) and SIAF- DST, Karnatak University Dharwad for spectral analyses.

References

1 Zuccolo M, Kunova A, Musso L, Forlani F, Pinto A, Vistoli G, Silvia G, Cortesi P & Dallavalle S, *Sci Rep*, 9 (2019) 11377.
2 Lopez-Moreno R, Mercader J V, Agullo C, Abad-Somovilla A & Abad-Fuentes A, *Org Biomol Chem*, 11 (2013) 7361.
3 Balba H, *J Environ Sci - Part B*, 42 (2007) 441.
4 Bartlett D W, Clough J M, Godwin J R, Hall A A, Hamer M & Parr-Dobrzanski B, *Pest Manag Sci*, 58 (2002) 649.
5 Correia M, Rodrigues M, Paiga P & Delerue-Matos C, *In: Encyclopedia of Food and Health*, (Elsevier) 2016, p. 169.
6 Balba H, J Environ Sci- Part B, 42 (2007) 441. (Same as reference number 3)
7 Lopez-Moreno R, Mercader J V., Agullo C, Abad-Somovilla A & Abad-Fuentes A, *Org Biomol Chem*, 11 (2013) 7361.
8 Shi Z, Wang F, Zhou W, Zhang P & Fan Y J, *Int J Mol Sci*, 8 (2007) 1001.
9 Liu C, Guan A, Yang J, Chai B, Li M, Li H, Yang J & Xie Y, *J Agric Food Chem*, 64 (2016) 45.
10 Zhang J, Zhu F, Gu M, Ye H, Gu L, Zhan L, Liu C, Yan C & Feng G, *Postharvest Biol Tech*, 181 (2021) 111675.
11 Al-Othmana M R, El-Aziz A R M A, Mahmoud M A, Eifan S A, El-Shikh M S & Majrashi M, Dig J NanomaterBiostruct 9 (2014) 151.
12 Vincent J M, *Nature*, 159 (1947) 850.
13 Dey U, Harlapur S I, Dhutraj D N, Suryawanshi P, Jagtap G P, Apet K T, Badgujar S L, Gholve V M, Kamble H N & Kuldh D P, 8 (2013) 4960.
14 Dinesh B M, Kulkarni S, Harlapur S I, Benagi V I & Mallapur C P, *Int J Plant Prot*, 8 (2015) 295.
15 Schüttelkopf A W & Van Aalten D M F, *Acta Crystallogr D BiolCrystallogr*, 60 (2004) 1355.
16 Tian W, Chen C, Lei X, Zhao J & Liang J, *Nucleic Acids Res*, 46 (2018) W363.
17 Morris G M, Huey R, Lindstrom W, Sanner M F, Belew R K, Goodsell D S & Olson A J, *J Comp Chem*, 30 (2009) 2785.
18 Trott O & Olson A J, *J Comp Chem*, 31 (2010) 455.
19 Jinadatta P, Rajshekarappa S, Rao S R K, Subbaiah S G P & Shastri S,. *BioImpacts*, 9 (2019) 239–249. https://doi.org/10.15171/bi.2019.29
20 Shastri S L, Krishna V, Ravi K S, Santosh K S R, Ramu V & Pradeepa K, *World J Pharm Sci*, 4 (2016) 331.
21 Gudimani P, Shastri SamundeeswariL, Pawar V, Shastri L A & Sungar V A, *Chem Data Collect*, 33 (2021) 100692.
22 Balba H, *J Environ Sci Part B*, 42 (2007) 441.
23 Bartett D W, Clough J M, Godfrey C R A, Godwin J R, Hall A A, Heaney S P & Maund S J, *Pesticide Outlook*, 12 (2001) 143.
24 Sun S, Yan J, Tai L, Chai J, Hu H, Han L, Lu A, yang C & Chen M, *Mol Divers*, 27 (2023) 145.
25 Sharma V, Shing B, Hernandez-Alvarez L, Debnath A & Podust L M, *Mol Pharmacol*, 98 (2020) 770.